Article

Synthesis and Characterization of Fe(III) Chitosan Nanoparticle N-Benzaldehyde Schiff Base for Biomedical Application

Gift Okunzuwa * , Omamoke Enaroseha , Samuel Okunzuwa

Posted Date: 17 July 2023

doi: 10.20944/preprints202307.1085.v1

Keywords: chitosan nanoparticle; Schiff base; complexation; antimicrobial agent; antibiotic sensitivity

Article

Synthesis and Characterization of Fe(III) Chitosan Nanoparticle N-Benzaldehyde Schiff Base for Biomedical Application

Okunzuwa Iyobosa Gift [1,*], Omamoke O. E. Enaroseha [2] and Okunzuwa Ikponmwosa Samuel [3]

[1] Department of Physics, Delta State University, Abraka, Nigeria
[2] Department of Physics, Delta State University of Science and Technology, Ozoro, Nigeria
* Correspondence: author: enarosehaomamoke@gmail.com; Iyobosa.iyawe@uniben.edu

Abstract: The present study produced and characterised chitosan, chitosan nanoparticle, chitosan n – benzaldehyde Schiff base, chitosan nanoparticle n – benzaldehyde Schiff base, Fe(III) chitosan n – benzaldehyde Schiff base and Fe(III) chitosan nanoparticle n – benzaldehyde Schiff base for biomedical application as antimicrobial agents. The materials were characterized with Fourier Transform Infrared spectroscopy, X-ray Diffractogram and biologically evaluated using disc diffusion method with three gram-positive bacteria. The FTIR absorption peaks were shifted to a lower wave number than the micro materials from which it was modified. These clearly indicate the linkage between phosphate, ammonium ion, Schiff base and Fe(III) metal. The diffracted peaks of Fe(III) chitosan nanoparticle n – benzaldehyde Schiff base were new peaks at $2\theta = 24^{o}$ and 42^{o} when compare to the peak of Fe(III) chitosan n – benzaldehyde Schiff base of $2\theta = 22.5^{o}$ and 34^{o}. The difference in peak shift were attributed to the ionic bonding of the complexation of Fe(III) with the blending of benzaldehyde to chitosan – Tpp backbone structure. Fe(III) chitosan nanoparticle Schiff base has more antimicrobial activity against same bacteria and fungi tested than Fe(III) chitosan n – benzaldehyde Schiff base, chitosan n – benzaldehyde Schiff base and chitosan. The antimicrobial activities of the synthesised six materials shown that the materials have high activities than the above – mentioned standard drugs.

Keywords: chitosan nanoparticle; Schiff base; complexation; antimicrobial agent; antibiotic sensitivity

1. Introduction

Schiff bases are versatile organic compounds which are widely used and synthesized by condensation of either an aldehyde or a ketone with a primary amine. The carbonyl group of the aldehyde gives aldimines while that of ketone gives ketoimines. They are condensation products of ketones (or) aldehydes with primary amines [1]. Hugo Schiff discovered Schiff base in 1864, by condensation reaction of alkanal or alkanone and primary in azeotropic distillation, which was named after him [2]. A large number of different Schiff base ligands have been used as cation carriers in potentiometric sensors as they have shown excellent selectivity, sensitivity, and stability for specific metal ions such as Ag(II), Al(III), Co(II), Cu(II), Gd(III), Hg(II), Ni(II), Pb(II), Y(III), and Zn(II) [3]. Schiff bases have been studied for their important properties in catalysis [4].

Chitosan, which is easily derived from chitin by N – deacetylation, has both hydroxyl and amino groups that can be modified easily. In recent years various research on the use of chitosan has drawn attention, especially for wastewater treatments [5]. Chitosan, essentially (1,4) – 2 – amino – 2 – deoxy-/3-D glucan, possesses an elevated chelating capacity, mainly due to the large amount of primary amino groups regularly distributed along the chains it presents [6]. Chitosan is a potentially useful material for cathode fabrication due to its low cost and abundance. Chitosan has been utilized in many applications as gels, films, or fibers, and particularly as a hydrogel absorbent for environmental contaminants due to its low cost and abundance.

 doi:10.20944/preprints202307.1085.v1

Recently, it is well known that nanoparticles are considered to be viable alternatives to antibiotics and seem to have an effective potency to solve the problem of the emergence of bacterial multidrug resistance. Super paramagnetic iron oxide (Fe_3O_4) is the most commonly used as drug delivery nanoparticles in biomedical applications due to its biocompatibility [7], biodegradability and simple surface modification [8]. One promising technique for nanoparticles surface modification is by coating the nanoparticles with polymers to avoid iron oxide oxidation. Some polymers used for Fe_3O_4 nanoparticles coating are polyethylene glycol (PEG), dextran, polyethylene imine (PEI), phospholipids, and chitosan. Natural polymers, such as chitosan, is highly recommended in the drug carrier systems, due to its biocompatibility and biodegradability characteristics [8]. Chitosan has the ability to interact with negatively charged (hydroxyl groups) on the surface of Fe_3O_4 nanoparticles. Chitosan, Schiff bases and metal complexes have been reported to have many antibacterial and antifungal properties, the results obtained by [9,10] and also because of increasing resistance of bacteria and fungi to available antimicrobials. [9] Prepared and characterized carboxymethyl chitosan Schiff base with different benzaldehyde which they applied on some bacteria and fungi. [10], synthesized, characterized chitosan 4 – chlorobenzaldehyde Schiff base which they applied on some bacteria and fungi from the results obtained, the antimicrobial activity was lesser than the standard drug during comparison. Owing to this findings, this study is concerned with the synthesis, characterization of chitosan, chitosan nanoparticle, chitosan n – benzaldehyde Schiff base, chitosan nanoparticle n – benzaldehyde Schiff base, Fe(III) chitosan n – benzaldehyde Schiff base and Fe(III) chitosan nanoparticle n – benzaldehyde Schiff base for biomedical application as antimicrobial agents.

1. Materials and Methods

All chemicals, in this study were used without further purification.

2.1. Preparation of chitosan from giant snail shell (Achatina marginata):

Snail shells were obtained from Effurun market, Warri in Nigeria. The snail shells were washed, soaked in warm water, dried and ground to powder. The grounded shells were later sieved with a mesh sieve (425 μm). Chitosan was prepared from the ground snail shells with slight modification according to the method described by [11].

Preparation of chitosan was through deproteinization, demineralization and deacetylation processes [11].

2.1.1. Deproteinization:

In this process the protein content of the shell is withdrawn from the main chemical structure, this process is done by treating the shells in an alkaline aqueous solution composed of sodium hydroxide [12].

2.1.2. Demineralization:

An organic matter specifically calcium carbonate ($CaCO_3$) is eliminated in dilute acidic medium. This is done by treating the shells in dilute HCl solution.

2.1.3. Decolourization:

This process is to remove natural pigment that existed in chitin [13].

2.1.4. Deacetylation:

This is a step to convert the chitin to chitosan. In more specific term, it is a process that involves partial removal of an acetyl group from chitin structure [14] it is normally involved with an alkaline bath [15].

Preprints (www.preprints.org) | NOT PEER-REVIEWED | Posted: 17 July 2023 doi:10.20944/preprints202307.1085.v1

2.2. Experimentals:

The ground snail shell (200 g) was put in a beaker and deproteinated by heating it in l.2 M sodium hydroxide (2.5 L) for 2½ hours at 80^{0}C, with occasional stirring. The mixture was allowed to cool and the excess sodium hydroxide solution decanted. The residue was washed with plenty of deionized water to neutral pH and air-dried. The air-dried sample was added to 0.7 M HC1 (760 mL) in a beaker, to remove the calcium carbonate. The excess HC1 was decanted and the residue washed with deionized water to a neutral pH, filtered and air–dried. The sample was further placed in 0.32% solution of sodium hypochlorite (1.2 L) in a beaker for 30 min, washed to neutral pH and air-dried. This gave chitin (l20.25 g). The chitin was put into a beaker and deacetylated with 50% sodium hydroxide (1.3 L) at a temperature of 121^{0}C for 80 min. The excess sodium hydroxide solution was decanted. The residue was washed to neutral pH with deionized water and air-dried to give chitosan powder.

2.3. Purification of chitosan

According to [16], Chitosan (1 g) was dissolved in acetic acid (2%) and left overnight. The solution was then filtered through cheesecloth to remove contaminant and un-dissolved particles. Chitosan was then precipitated with 5% sodium hydroxide, collected and washed with distilled water to remove excess of alkali.

2.4. The degree of deacetylation [17]

The degree of deacetylation refers to the removal of an acetyl group from the chain. This is determined by the titrimetric method, chitosan solution (1%) prepared using acetic acid was added to phosphoric acid in the ratio of 1:1(V/V) and the mixture was titrated against 0.1 M NaOH using phenolphthalein as an indicator. The degree of deacetylation can be obtained using the following formula:

$$100 - 2.303\ \frac{v_1 - v_0}{m} \tag{1}$$

where **m** is the amount of chitosan (g), $\mathbf{V_1}$ is the final volume (mL), and $\mathbf{V_0}$ is the initial volume (mL)

2.5. Preparation of chitosan nanoparticle:

For the preparation of chitosan nanoparticle through ionic gelation, the method of [18] was used.Chitosan 0.5% (w/v) was dissolved with acetic acid 1% (v/v) and then increased to pH 4.6 – 4.8 with 2 M NaOH. Chitosan nanoparticles were formed spontaneously upon addition of an aqueous tripolyphosphate solution (1mL) of 0.25% (w/v) to chitosan solution (3mL) under magnetic stirring of 1000 rpm for 1 hour at room temperature. The nanoparticles were purified by centrifugation at 16000 rpm for 30 min. The supernatants were discarded and the chitosan nanoparticles were extensively rinsed with distilled water to remove any sodium hydroxide and then freeze-dried.

For chitosan n – benzaldehyde Schiff base through coupling, we use the method described by [19,20]. 1.0 g of Chitosan was dissolved in 50 mL of acetic acid 2% and stirred at room temperature for 6 hours. 10 mL of ethanol containing 0.0695g of benzaldehyde was added to the solution with stirring to form a homogenous solution. The mixture was stirred for 6 hours and heated at 50^{0}C. A deep yellow gel indicating the formation of Chitosan Schiff base was obtained. The product was cooled and washed with distilled water and ethanol several times to remove unreacted benzaldehyde until colourless filtrate was obtained. The product was then dried at 50^{0}C in vacuum for 24 hours.

For [21], the preparation of Chitosan nanoparticles n – benzaldehyde Schiff-base (CNSB) is as follow: 1.0 g of Chitosan was added to 100 mL of ethanol and the mixture was continuously stirred for 6 hours to produce a homogeneous solution. Afterwards, 0.0695g of benzaldehyde was added to the mixture. The obtained mixture was further stirred for 6 hours at 50^{0}C. Chitosan nanoparticle Schiff base formed was separated by centrifugation at 16000 rpm and washed several times with ethanol.

 doi:10.20944/preprints202307.1085.v1

The product was dried in a vacuum oven at 50^0C for 24 hours; a yellow powder of chitosan nanoparticle Schiff base was obtained.

2.6. Synthesis of Fe(III) chitosan:

Synthesis of Fe(III) chitosan n – benzaldehyde Schiff base through complexation follows the method of [19]. 1.0 g Chitosan n – benzaldehyde Schiff base was mixed with 1.0 g Iron (III) chloride in 50 mL ethanol solution, stirred and heated at 50^0C for 12 hours in water bath. After cooling, the crude complex was washed with ethanol and subsequently washed to colourlessness by excess amounts of water, and then dried at 50°C in an oven for 24 hours.

2.7. Characterisation:

Materials were analyzed with Fourier Transform Infrared (FTIR) Spectroscopy using KBR pellet method and recorded in the frequency range of 400 – 4000 cm^{-1} with model Cary 630 by Agilent technologies. USA and X-ray diffractograms of samples were obtained using an X-ray powder diffractometer (a Bruker AXS model, Germany) with Ni-filter and CuKα radiation source at an accelerating voltage/current of 50 KV/40 mA. The relative intensity was recorded in the scattering rage, varying from 5^0 to 90^0 at scanning rate 2^0min^{-1}.

2.8. Evaluation of antimicrobial activities:

The evaluation of antimicrobial activities of the synthesized materials through the agar disk diffusion method [22].

2.8.1. Preparation of materials / samples concentration:

Chitosan, chitosan nanoparticle, chitosan n – benzaldehyde Schiff base, chitosan nanoparticle n – benzaldehyde Schiff base, Fe(III) chitosan n – benzaldehyde Schiff base and Fe(III) chitosan nanoparticle n-benzaldehyde Schiff base used in this study were dissolved each in diméthylsulfoxyde (DMSO) to obtain varying concentrations (100%, 50% and 25%). Then, a concentration of 100% was achieved by dissolving 1g of the material in 1 mL of DMSO in a sterile universal bottle, 50% concentration was achieved by aseptically pipetting 0.5 mL of the 100% concentration and dissolving with 0.5 mL of DMSO and 25% concentration of each sample was achieved by dissolving 0.5 mL of the 50% concentration with 0.5 mL of DMSO.

2.8.2. Antibiotic Sensitivity Test:

The bacteria isolates were tested for resistance and sensitivity to different antibiotics using the standard disc diffusion method. The disc diffusion assay, bacteria were grown between 18 and 24 hours, while fungi were grown for 2-5 days on Mueller Hinton agar. The inoculated medium was maintained at 37^0C. The results were recorded after 24 hours and 2-5 days respectively. Standard antibiotics (oxoid) were used to determine the resistance pattern of the isolates. The diameters of the zone of inhibition around each disc were measured using a meter rule. Gram-positive and Gram-negative antibiotics sensitivity disc used in the study include Meropenem (10 ug), Gentamicin (30 ug), Vancomycin (30 ug), Amoxicillin/ Clavulanic Acid (30 ug), Ciprofloxacin (5 ug), Sulfamethoxazole/ Trimethoprim (25 ug), Ceftazidime (30 ug), Erythromycin (15 ug). For fungi Fluconazole (30 ug) was used. The antibiotics discs served as positive control.

2.8.3. Antibacterial and Antifungal Activity of the Materials:

Screening of the materials Chitosan, Chitosan nanoparticle, Chitosan n – benzaldehyde Schiff base, Chitosan nanoparticle n – benzaldehyde Schiff base, Fe(III) chitosan n – benzaldehyde Schiff base and Fe (III) chitosan nanoparticle n – benzaldehyde Schiff base for antimicrobial activity was carried out by disc diffusion method which is normally used as a preliminary check and to select between efficient materials. The tests were conducted with the authenticated pure culture of the

Preprints (www.preprints.org) | NOT PEER-REVIEWED | Posted: 17 July 2023 doi:10.20944/preprints202307.1085.v1

tested pathogens to determine their respective susceptibility or resistance to the materials. Sterile agar plates were aseptically inoculated with a loop full of the test bacteria and fungi. Each inoculum was spread evenly over the surface of the agar plate. Under aseptic conditions empty sterile disc (Whatman filter paper no. 5, 6 mm diameter) were impregnated with 1000 uL of different concentrations (100%, 50% and 25%) of each of the materials and placed on the agar surface. Paper disc moistened with DMSO, was placed on the seeded plates as a negative control. The plates were left for 30 mins at room temperature to allow the diffusion of the materials and then they were incubated at 37^0C for 24hours at a pressure of 15 psi for bacteria and 2-5 days for fungi. The plates were observed for the presence of the inhibition zone around the disc. The extent of inhibition was determined by measuring the diameter of the inhibition zone using the transparent meter rule. Measurements were made across the discs.

3. Results and discussion:

3.1. Degree of deacetylation of chitosan:

The Degree of deacetylation is used to establish that chitosan has been successfully prepared before further analysis. The degree of deacetylation of the prepared Chitosan was 90.1%. This is a calculated measure of the extent of conversion of acetyl groups in chitin to amine groups of Chitosan. The properties of Chitosan are strongly dependent on the degree of N – deacetylation of chitin. This is an essential factor for the study of its structure-property relationship. The result above is in agreement with the reports of other researchers that chitin with a degree of deacetylation above 50% can be considered as Chitosan [13,23].

3.2. Ionic interaction between Chitosan and Tripolyphosphate (TPP):

The reaction of Chitosan with tripolyphosphate (TPP) leads to the formation of intermolecular and/or intramolecularnetwork structure by ionic interaction between NH_3^+ protonated groups and negatively charged ions OH^- and $P_3O_{10}^{5-}$ of tripolyphosphate. Due to hydrolysis, the small molecules of polyelectrolyte, sodium tripolyphosphate, dissociates in water and released out OH^- ions. At pH values of 4.8, the interaction mechanism is ionic crosslinking, as shown in Figure 1

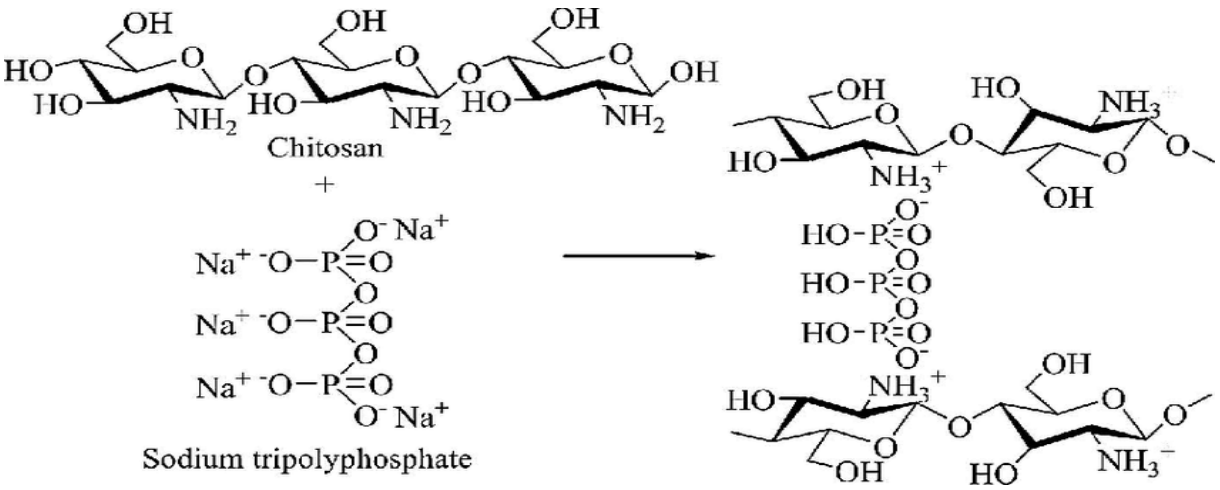

Figure 1. Ionic crosslinking interaction mechanisms between Chitosan and Tripolyphosphate (TPP).

The preparation of chitosan Schiff base deals with the coupling of chitosan primary amine group with benzaldehyde active carbonyl group to produce an imine group, which gave deep yellow powdered Schiff base as presented in the reaction scheme in Figure 2.

Preprints (www.preprints.org) | NOT PEER-REVIEWED | Posted: 17 July 2023 doi:10.20944/preprints202307.1085.v1

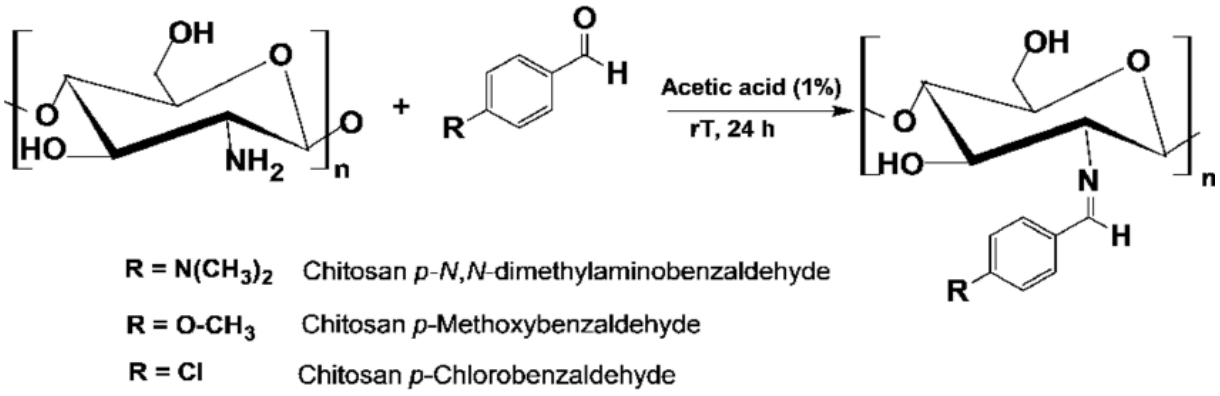

Figure 2. Condensation reaction of chitosan with n-Benzaldehyde to form chitosan Schiff base.

3.3. Complexation of chitosan n-benzaldehyde Schiff base with metal ion:

The prepared chitosan Schiff base was complexed with Fe^{3+} to form chitosan Schiff base Fe^{3+} complex which was brown in colour.

3.4. Physical appearances of the synthesized materials:

The physical appearances of the compounds were noted by visual observation. The materials obtained were brown and deep yellow powdered solids as presented in Table 1 except for chitosan and chitosan nanoparticles which were off-white and white respectively.

Table 1. Physical characteristics of the synthesized materials.

Materials	Colour
Chitosan	Off-white
Chitosan nanoparticle	White
Chitosan n-benzaldehyde Schiff base	Deep yellow
Chitosannanoparticlen-benzaldehydeSchiff base	Deep yellow
Fe (III) Chitosan n-benzaldehyde Schiff base	Brown
Fe (III) Chitosannanoparticlen-benzaldehydeSchiff base	Brown

3.5. Data Analysis:

It is mandatory to determine the structure and properties of the synthesized materials in order to know the specific functional groups, chemical bonds that exist in a material, surface and structural morphology, including particle size and crystalline nature.

3.6. Fourier Transform Infrared(FTIR)Spectroscopy:

The important FTIR spectroscopy results confirm the formation of all the prepared materials for chitosan, chitosan nanoparticle, chitosan n – benzaldehyde Schiff base, chitosan nanoparticle n – benzaldehyde Schiff base, Fe(III) chitosan n – benzaldehyde Schiff base and Fe(III) chitosan nanoparticle n – benzaldehyde Schiff base.

The spectrum of Chitosan in Figure 3, shows a broad band at 3347.1 cm^{-1} which is due to the intermolecular hydrogen bond OH and NH stretching. The band at 1640 cm^{-1} is assigned to the NH bending (NH_2) while the peaks at 1148.0 cm^{-1} and 894.6 cm^{-1} are attributed to β (1→4) glycosidic bridge and CH_2 bending due to pyranose ring. The band at 1062.3 cm^{-1} is attributed to C-O stretching.

From Figure 4, it was observed in the spectrum of Chitosan- Tpp nanoparticle that peaks shifted to lower wave number when compared to the spectrum of Chitosan. The characteristics absorption peaks of chitosan at 3347.1 $cm^{-1}$and 1640 $cm^{-1}$of V(OH) and V(NH_2) respectively, were shifted to a lower wavenumber of 3056.4 cm^{-1} and 1636 cm^{-1}in chitosan- Tpp nanoparticle spectrum.

Preprints (www.preprints.org) | NOT PEER-REVIEWED | Posted: 17 July 2023 doi:10.20944/preprints202307.1085.v1

Moreover, these bands in chitosan-tpp nanoparticles were broader and stronger. The peaks at 1151.7 cm^{-1} and 1215.1 showed the presence of P=O and P-O groups respectively which was not present in the spectrum of Chitosan.This is an evidence of molecular interaction between the NH_3^+ protonated groups of chitosan and negatively charged Sodium tripolyphosphate (TPP) [24].

The Infrared spectrum of chitosan n-benzaldehyde Schiff base in Figure 5, exhibit main characteristics strong broad band at 3350.8 cm^{-1}which correspondsto stretching vibration of N-H and O-H groups of chitosan. The spectrum clearly shows the interaction between the chitosan matrix and the benzaldehyde through the formation of an imine group which was confirmed by the peak at 1631.0 cm^{-1}. The shift in peaks observed in the blendof chitosan with benzaldehydewhen compared with the FTIR spectrum of pure chitosanis as a result of the formation of chitosan Schiff base. The characteristic band observedat 1558.0 $cm^{-1}$is attributed to the aromatic ring (C=C) of the benzaldehyde in the Schiff base [20,25].

From Figure 6, it was observed that the spectrum of Chitosan nanoparticle n – benzaldehyde Schiff base was different from that of Chitosan n – benzaldehyde Schiff base. The absorption peaks of Chitosan n – benzaldehyde Schiff base at 3350 cm^{-1}, 1631.0 cm^{-1} and 1558.0 cm^{-1} of OH stretching vibration, C=N vibration and aromatic ring (C=C) respectively were shifted to a lower wavenumber at 3283.8 cm^{-1}, 1621.3cm^{-1} and 1524.5cm^{-1} in Chitosan nanoparticle Schiff base. These clearly indicate the interaction between chitosan – Tpp nanoparticle amine group at the N – position and n – benzaldehyde in the formation of chitosan nanoparticle n- benzaldehyde Schiff base [21].

The spectra of Fe(III) chitosan n – benzaldehyde Schiff base in Figure 7, shows similar spectra as that of chitosan n – benzaldehyde Schiff base but with few differences (changes). It is observed that the C=N (imine) stretching band of Fe(III) chitosan n – benzaldehyde Schiff base is shifted to a lower wave number at 1625.1 cm^{-1}. This may be due to the co-ordination of Fe(III) metal centre with azomethine nitrogen atom. The absorption peak at 678.4 cm^{-1} is assigned to ionic Cl^- ($FeCl_3$) that was used in the complexation reaction. This shows that Cl^- existed in the complex in an ionic form. This is in agreement with [26].

From Figure 8, it was observed that the spectrum of Fe(III) Chitosan nanoparticle n – benzaldehyde Schiff base was different from that of Fe(III) Chitosan n – benzaldehyde Schiff base. The absorption peaks of Fe(III) Chitosan Schiff base at 1625.0cm^{-1} and 678.4cm^{-1} of C=N (imine) vibration and Cl^- respectively was shifted to a lower wavenumber at 1616.3 cm^{-1} and 682.1cm^{-1}in Fe(III) Chitosan nanoparticle n – benzaldehyde Schiff base. These clearly indicate the interaction between chitosan – Tpp nanoparticle n – benzaldehyde Schiff base and Fe^{3+}in the formation of Fe(III) chitosan nanoparticle n – benzaldehyde Schiff base.

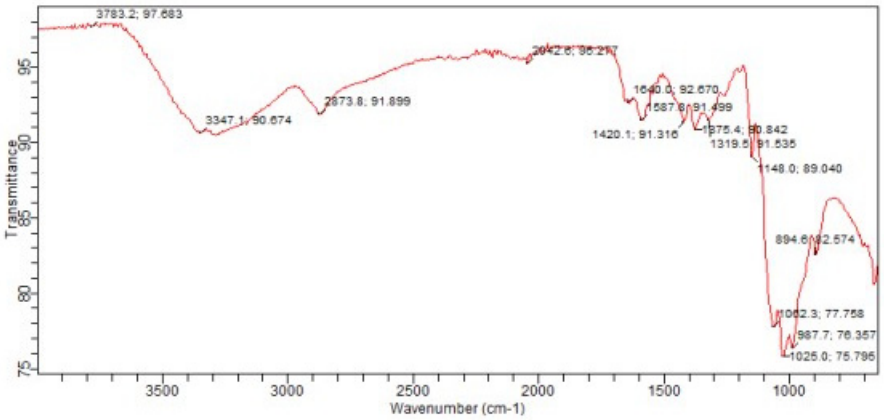

Figure 3. FTIR spectra of Chitosan.

Preprints (www.preprints.org) | NOT PEER-REVIEWED | Posted: 17 July 2023 doi:10.20944/preprints202307.1085.v1

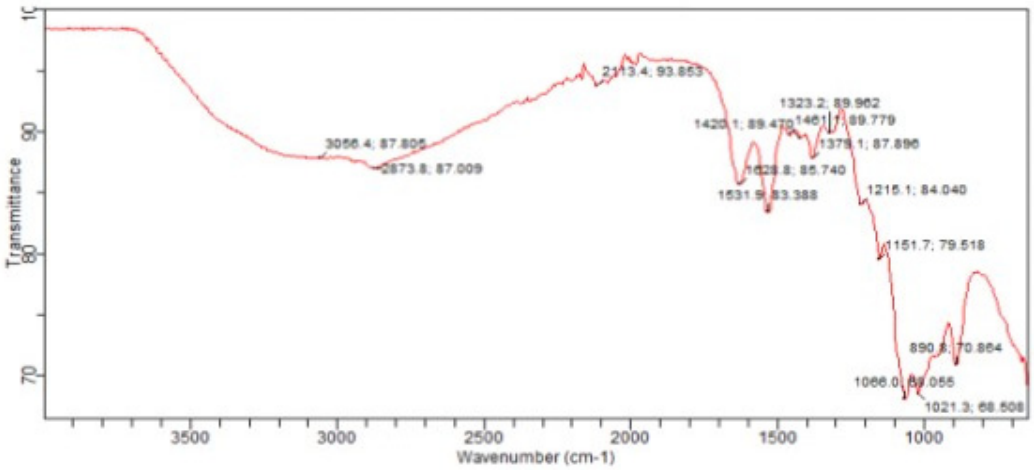

Figure 4. FTIR spectra of Chitosan nanoparticle.

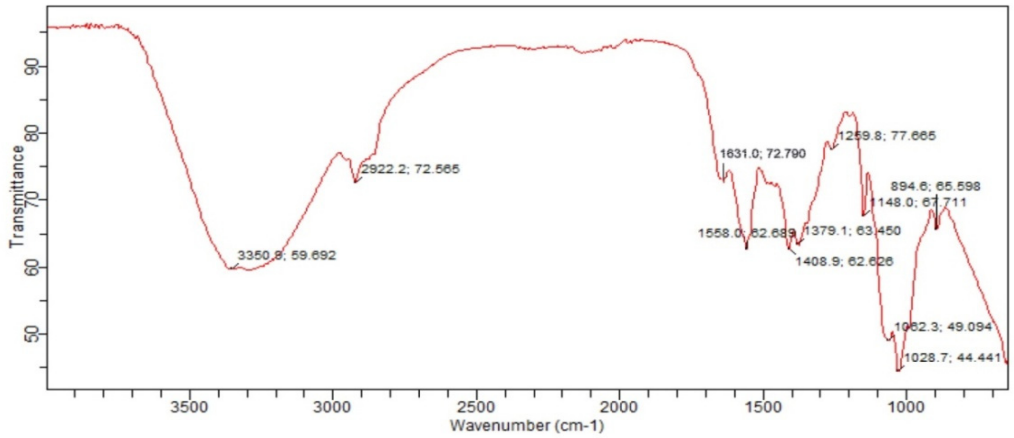

Figure 5. FTIR spectra of Chitosan n-benzaldehyde Schiff base.

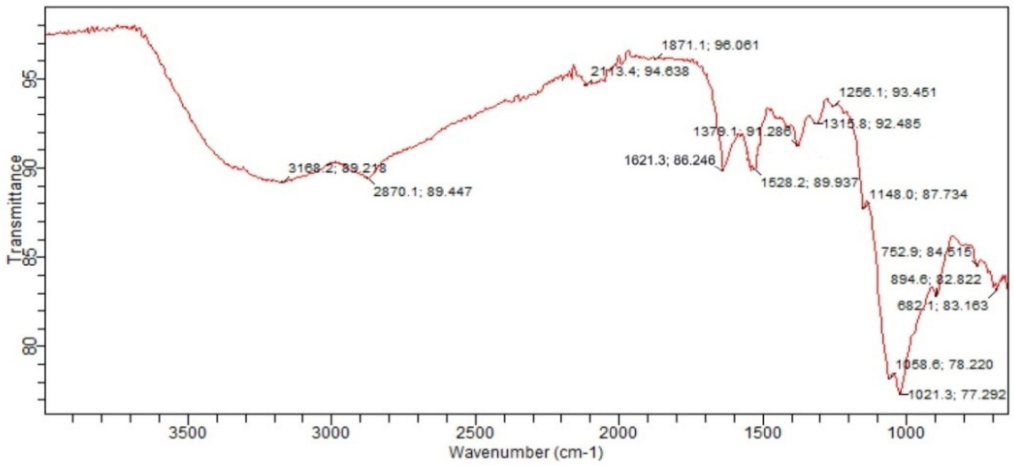

Preprints (www.preprints.org) | NOT PEER-REVIEWED | Posted: 17 July 2023 doi:10.20944/preprints202307.1085.v1

Figure 6. FTIR spectra of Chitosan Nanoparticle n-benzaldehyde Schiff base.

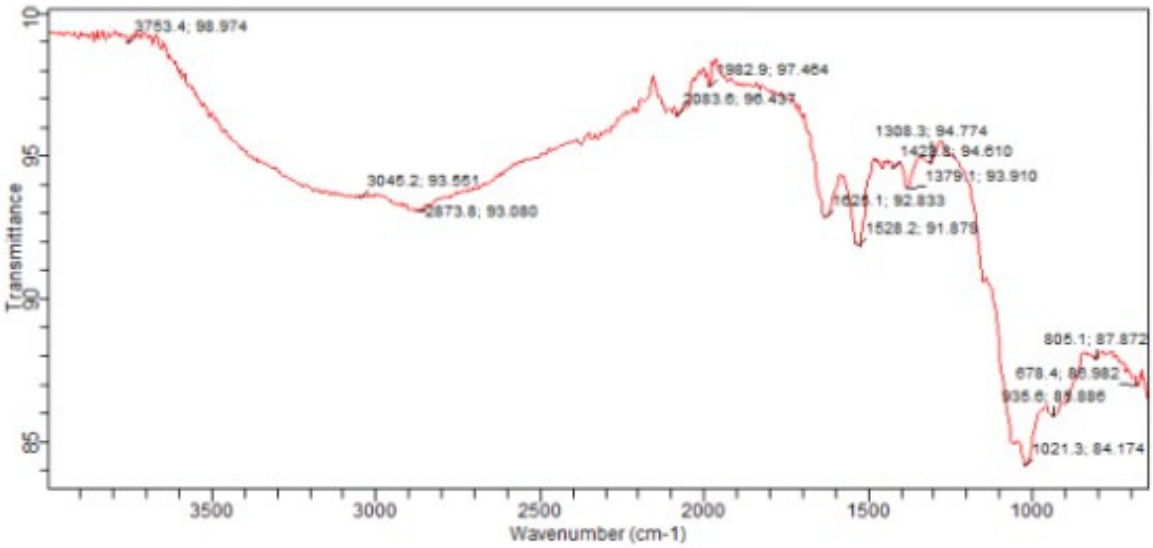

Figure 7. FTIR spectra of Fe(III) Chitosan n-benzaldehyde Schiff base.

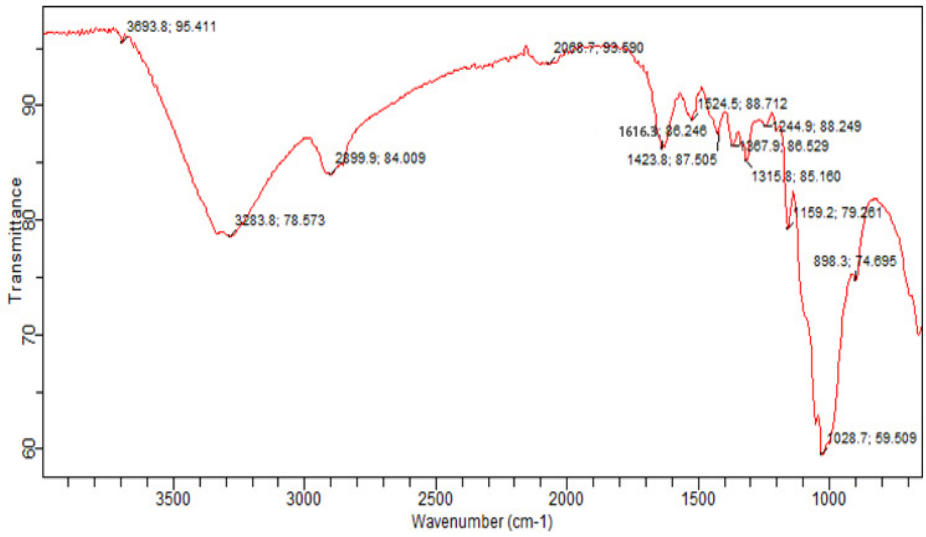

Figure 8. FTIR spectra of Fe(III) Chitosan nanoparticle n-benzaldehyde Schiff base.

3.7. X-ray diffractogram (XRD):

The XRD difractogram was used to determine the structural morphology and phase identification of the materials produced. The XRD pattern is measured in 2θ degree due to Bragg's equation ($n\lambda = 2d \sin\theta$). The incident ray and reflected ray all making the angle θ with crystal plane. Reflections from planes set at θ angle with respect to the incident beam generate a reflected beam at an angle 2θ from the incident beam. The XRD pattern results for Chitosan, Chitosan nanoparticle, Chitosan n – benzaldehyde Schiff base, Chitosan nanoparticle n-benzaldehyde Schiff base, Fe(III) chitosan n – benzaldehyde Schiff base and Fe(III) chitosan nanoparticle n – benzaldehyde Schiff base are presented in Table 8 and Figures 10–15 respectively.

Preprints (www.preprints.org) | NOT PEER-REVIEWED | Posted: 17 July 2023 doi:10.20944/preprints202307.1085.v1

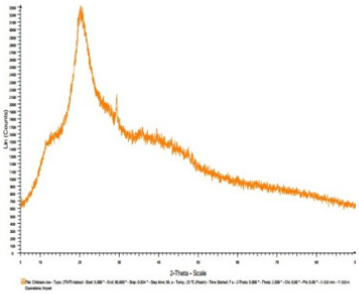

File: Chitosan. raw -Type: 2Th/Th Locked - Start 5.000° - End: 90.000° - Step: 0.034°- Step time: 96.s - Temp: 25°C (Room) -Time started: 7 s - 2-Theta 5.000° - Theta: 2.500° - Chi: 0.00° - Phi: 0.00°- X: 0.00° - Y: 0.0 m Operations: Import.

Figure 9. XRD pattern of Chitosan.

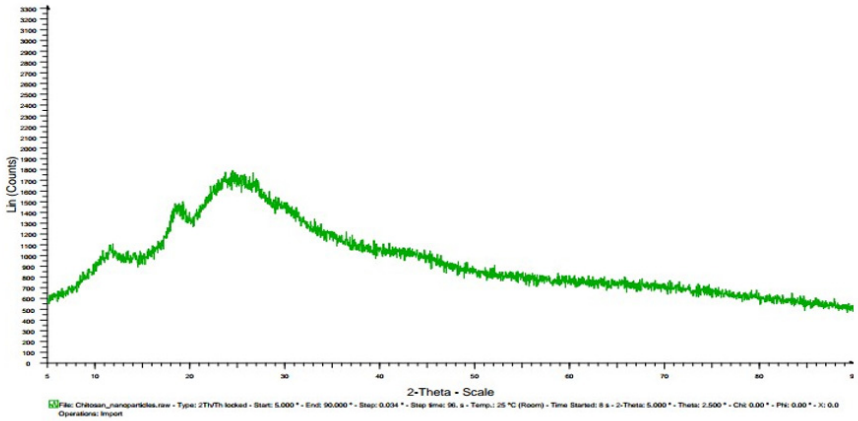

File: Chitosan nanoparticles. raw -Type: 2Th/Th Locked - Start 5.000° - End: 90.000° - Step: 0.034°- Step time: 96.s - Temp: 25°C (Room) -Time started: 8 s - 2-Theta 5.000° - Theta: 2.500° - Chi: 0.00° - Phi: 0.00°- X: 0.00° - Y: 0.0 m Operations: Import.

Figure 10. XRD Pattern of Chitosan Nanoparticle.

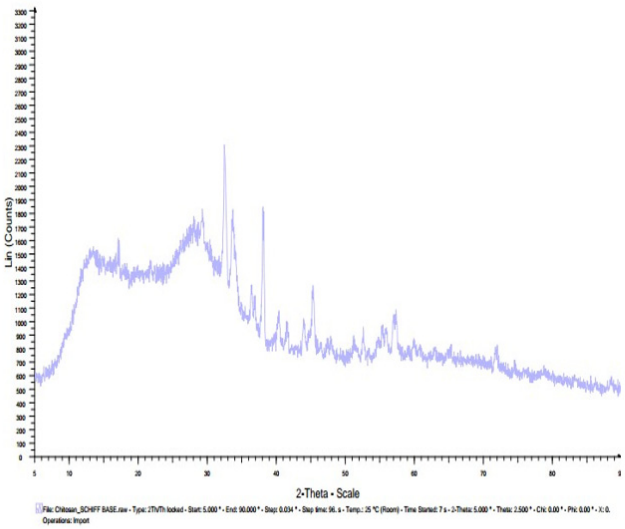

File: Chitosan_ SCHIFF BASE. raw -Type: 2Th/Th Locked - Start 5.000° - End: 90.000° - Step: 0.034°- Step time: 96.s - Temp: 25°C (Room) - Time started: 7 s - 2-Theta 5.000° - Theta: 2.500° - Chi: 0.00° - Phi: 0.00°- X: 0.00° - Y: 0.0 m Operations: Import.

Figure 11. XRD Pattern of Chitosan n – benzaldehyde Schiff base.

Preprints (www.preprints.org) | NOT PEER-REVIEWED | Posted: 17 July 2023 doi:10.20944/preprints202307.1085.v1

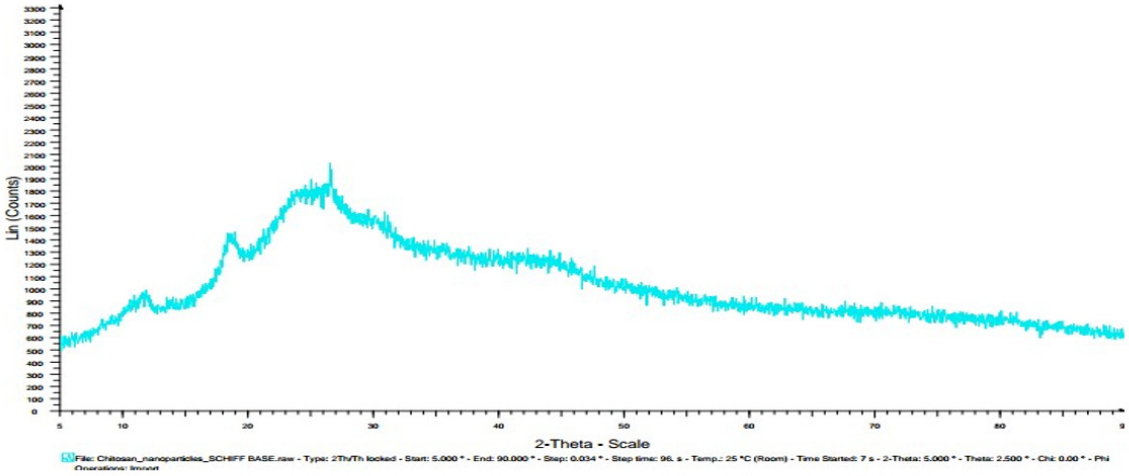

File: Chitosan_nanoparticles_SCHIFFBASE. raw -Type: 2Th/Th Locked - Start 5.000° - End: 90.000° - Step: 0.034°- Step time: 96.s - Temp: 25°C (Room) -Time started: 7 s - 2-Theta 5.000° - Theta: 2.500° - Chi: 0.00° - Phi: 0.00°- X: 0.00° - Y: 0.0 m Operations: Import.

Figure 12. XRD Pattern of Chitosan Nanoparticle n – benzaldehyde Schiff base.

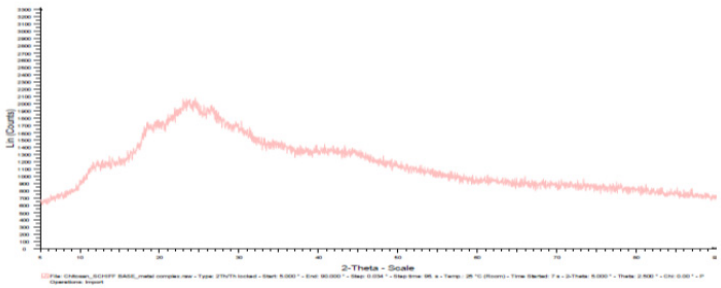

File: Chitosan_ SCHIFF BASE_metalcomplex.raw -Type: 2Th/Th Locked - Start 5.000° - End: 90.000° - Step: 0.034°- Step time: 96.s - Temp: 25°C (Room) -Time started: 7 s - 2-Theta 5.000° - Theta: 2.500° - Chi: 0.00° - Phi: 0.00°- X: 0.00° - Y: 0.0 m Operations: Import.

Figure 13. XRD Pattern of Fe(III) Chitosan n – benzaldehyde Schiff base.

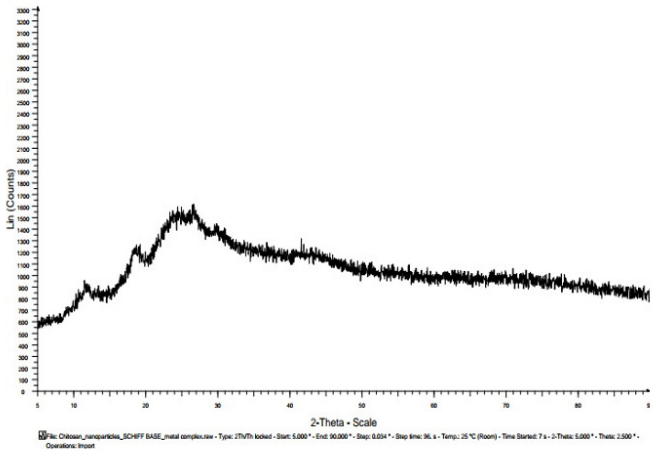

File: Chitosan_nanoparticles SCHIFF BASE_metalcomplex.raw -Type: 2Th/Th Locked - Start 5.000° - End: 90.000° - Step: 0.034°- Step time: 96.s - Temp: 25°C (Room) -Time started: 7 s - 2-Theta 5.000° - Theta: 2.500° - Chi: 0.00° - Phi: 0.00°- X: 0.00° - Y: 0.0 m Operations: Import.

Figure 14. XRD Pattern of Fe(III) Chitosan nanoparticle n – benzaldehyde Schiffbase.

The X – ray diffractogram of pure chitosan in Table 2 and Figure 9 has two main diffraction peaks: a weak diffraction peak at $2\theta = 11.5^0$ and a sharp diffraction peak $2\theta = 20^0$. This coincides with

Preprints (www.preprints.org) | NOT PEER-REVIEWED | Posted: 17 July 2023 doi:10.20944/preprints202307.1085.v1

the pattern of the tendon hydrate polymorph of chitosan. The sharp diffraction peak indicates a high crystalline nature of chitosan which infer high degree of crystallinity. This suggests the formation of inter and intramolecular hydrogen bonds in the presence of free amino groups in chitosan resulting in close molecular packing. This crystalline property of chitosan distinguishes it from most other carbohydrate polymers. This X-ray diffractogram pattern of chitosan is in accordance with the report of other researchers [10,22,26]. The XRD pattern of chitosan is compared with the XRD pattern of chitosan nanoparticle from Table 2, Figures 9 and 10. It was observed that the X-ray diffractogram of chitosan nanoparticle has new and many peaks when compared to the X-ray diffractogram of chitosan. The peaks at $2\theta = 19^0$ is smaller than that of chitosan at $2\theta = 20^0$, also chitosan nanoparticle has a weak and broad peak at $2\theta = 26^0$, showing a decrease in the crystalline nature of chitosan nanoparticle. This structural modification suggests that the intermolecular and/or intramolecular network structure of chitosan is crosslinked to each other by TPP (tripolyphosphate) counterions. These TPP counter ions interpenetrating the polymer chains of chitosan can imply certain disarray in the chain alignment and consequently results in decrease in crystallinity of chitosan-TPP nanoparticles material [24]. The X-ray diffractogram of chitosan n-benzaldehyde Schiff base in Table 2 and Figure 11 showed two peaks which are shifted to a higher 2θ value than that of Chitosan. The two peaks of chitosan n – benzaldehyde Schiff base are $2\theta = 14^0$ and 28^0. The diffraction peak at $28^0$is slightly broader than that of chitosan at $2\theta = 20^0$ and less intense. This suggests a decrease in crystallinity (semi crystalline) of the material due to the introduction of benzene ring. This is presumably the deformation of the strong hydrogen bond in the chitosan backbone with the substitution of benzaldehyde on the N- atom of chitosan. The intensity changes and peak shift in the X-ray diffractogram pattern of chitosan n – benzaldehyde Schiff base indicates good interactions which have taken place between chitosan and n – benzaldehyde during blending/ coupling of the material. The XRD pattern of chitosan n – benzaldehyde Schiff base is compared with the XRD pattern of chitosan nanoparticle n – benzaldehyde Schiff base here. From Table 2, Figures 11 and 12, it was observed that the chitosan nanoparticle n – benzaldehyde Schiff base X – ray diffractogram has new peaks at $2\theta = 12^0$, 19^0, 25^0, and 30^0 when compared to the X – ray diffractogram of chitosan n – benzaldehyde Schiff base peak at 14^0 and 28^0. The shifted diffraction peaks of chitosan nanoparticle n – benzaldehyde Schiff base at $2\theta = 12^0$, 19^0 and 25^0 is as a result of the inclusion of benzene in the Chitosan – TPP backbone structure. The diffracted shifted peaks were broad, large and supplementary. This suggests less homogeneity of the material resulting in amorphous nature. The X – ray diffractogram peaks of Fe(III) chitosan n – benzaldehyde Schiff base in Table 2 and Figure 13 showed that the diffracted peaks of Fe(III) chitosan n – benzaldehyde Schiff base were broad and weakened at $2\theta = 11.5^0$, 18.5^0, 22.5^0, 27^0, 34^0. This suggests a further decrease in crystallinityof the material. There was disappearance of some peaks and appearance of some new peaks when compared to the X-ray diffractogram of chitosan and chitosan n – benzaldehyde Schiff base. The intensity change of peaks may be due to the complexation of Fe^{3+} ion to chitosan Schiff base (imine group HC=N) matrix and to some extend spacial hinderance and hydrophobic force. The XRD pattern of chitosan is compared with the XRD pattern of chitosan nanoparticle here. From Table 2 and Figures 13 and 14, it was observed that there were few differences between the X – ray diffractogram of Fe(III) chitosan n-benzaldehyde Schiff base and Fe(III) chitosan nanoparticle n – benzaldehyde Schiff base. However, the differences in the diffracted peaks of Fe(III) chitosan nanoparticle n – benzaldehyde Schiff base are new peaks at $2\theta - 24^0$ and 42^0 when compare to Fe(III) chitosan n-benzaldehyde Schiff base at $2\theta - 22.5^o$ and 34^o. The difference in peak change may be attributed to the ionic bonding of the complexation of Fe(III) with chitosan – TPP n – benzaldehyde Schiff base backbone structure leading to amorphous nature of Fe(III) chitosan nanoparticle n – benzaldehyde Schiff base.

Table 2. The XRD patterns results for Chitosan, Chitosan nanoparticle, Chitosan n – benzaldehyde Schiff base, Chitosan nanoparticle n – benzaldehyde Schiff base, Fe(III) chitosan n – benzaldehyde Schiff baseand Fe(III) chitosan nanoparticle n – benzaldehyde Schiff base.

Materials	Diffracted Peaks at 2θ (Degree)

 doi:10.20944/preprints202307.1085.v1

Chitosan	11.5, 20
Chitosannanoparticle	12, 19,26,30
Chitosan n – benzaldehyde Schiff base	14, 28
Chitosannanoparticle n – benzaldehydeSchiff base	12, 19, 25, 27,30
Fe(III) Chitosan n – benzaldehyde Schiff base	11.5,18.5, 22.5, 27, 34
Fe(III) Chitosannanoparticlen – benzaldehydeSchiff base	12, 18.5, 24, 27, 42

3.8. Antibacterial assessment of all the synthesized materials:

The antimicrobial activities of chitosan, chitosan nanoparticle, chitosan n – benzaldehyde Schiff base, chitosan nanoparticle n – benzaldehyde Schiff base, Fe(III) chitosan n – benzaldehydeSchiff base and Fe(III) chitosan nanoparticle n – benzaldehydeSchiff base were investigated using varying concentrations (100%, 50% and 25%) labelled A, B and C respectively. The antimicrobial activities were evaluated using disc diffusion method; the zone of inhibition was measured with a transparent meter rule (mm). Measurements were made across the disc.

3.9. The experimental results of antimicrobial activity of all the materials using the inhibition zone method:

The antimicrobial activities of chitosan, chitosan nanoparticle, chitosan n – benzaldehyde Schiff base, chitosan nanoparticle n – benzaldehyde Schiff base, Fe(III) chitosan n – benzaldehyde Schiff base and Fe(III) chitosan nanoparticle n – benzaldehyde Schiff base with varying concentrations of 100%, 50%, 25% on three Gram positive bacteria: *Bacillus Subtilis*, *Bacillus cereus* and *Staphylococcus aureus*, two Gram-negative bacteria: *Samolena* and *Pseudomonas aeruginosa* and two fungi: *Candida albicans* and *Aspergillus niger* as shown in plates 3.8 – 3.10, each spot on the plates represents each material. In a typical experiment, the inhibition zone results were recorded after 24 hours of incubation at 37^0C for bacteria and 3 days of incubation at 37^0C for fungi. The obtained experimental data are clearly shown in Tables 9–15.

Tables 3 and 4 shows the antimicrobial activity trend of a high broader spectrum activity, higher inhibition and killing rate of the organisms: *Bacillus subtilis and Bacillus cereus* to be of the order of Chitosan nanoparticle < chitosan nanoparticle n-benzaldehyde Schiff base <Fe(III) chitosan nanoparticle n-benzaldehyde Schiff base, with inhibition zones ranging from 12mm – 18mm for *Bacillus subtilis*, 16mm – 26mm for *Bacillus cereus*at the highest concentration 100%. It was observed that the 100% concentration has the highest inhibition zone when compared to 50% and 25% concentrations, this is because the 100% concentration contains more active material of each sample than the 50% and 25% concentration. The activities of Fe(III) chitosan nanoparticle Schiff base may be attributed to the structural characteristics of Fe(III) Chitosan nanoparticle Schiff base which is the chelation of the metal ion (Fe(III)) unto the condensation of imine group of chitosan – tpp Schiff base, the enhanced result of the nanoparticle is because of its ease in reaching the target sites of the organism, increase in positive charge density, hydrophilicity, better solubility of the materials in aqueous media of the organism, suppression of spore elements and binding to essential nutrients needed for microbial growth and also the enhanced adsorption of polycation onto the negatively charged cell surface of the micro-organisms [22]. Tables 5 and 6 shows the antimicrobial activities of the organisms: *Staphylococcus aureus and Samolena* with the increasing concentrations (25%, 50% and 100%)of each material solutions of Chitosan nanoparticle < chitosan nanoparticle n – benzaldehyde Schiff base < Fe(III) chitosan nanoparticle n – benzaldehyde Schiff base. For *Staphylococcus aureus* with inhibition zones ranging from 16mm, 20mm and 24mm and for *Samolena* 0mm, 16mm and 18mm at different concentrations of 25%, 50% and 100% respectively.These activities is be attributed to the structural characteristics of Fe(III) Chitosan nanoparticle n – benzaldehyde Schiff base which is the chelation of the metal ion (Fe(III)) unto the condensation of imine group of chitosan – tpp n – benzaldehyde Schiff base and good surface contact of the molecules of the material. The antimicrobial activity observed in Table 7 against *Pseudomonas aeruginosa*,showed higher activity in chitosan nanoparticle and chitosan than in chitosan n – benzaldehyde Schiff base, chitosan nanoparticle n – benzaldehyde Schiff base, Fe(III) chitosan n – benzaldehyde Schiff base and Fe(III) chitosan

 doi:10.20944/preprints202307.1085.v1

nanoparticle n – benzaldehyde Schiff base, ranging from 00mm – 16mm. This may be attributed to the polycationic structure of chitosan which has led to the electrostatic interactions with the negative charges of the anionic components of the surface of the cell membranes of the bacteria (-COO^- or PO_4^{3}) groups. The interactions between positively charged chitosan molecules and negatively charged residues on the bacteria cell surface are considered to play an important role in the antimicrobial activity of Chitosan. The differences in cell surface electronegativity have led to the difference in the susceptibility of microbial cells towards Chitosan and Chitosan nanoparticle molecule [27].Tables 8 and 9, shows the antimicrobial activity of low inhibition zones for chitosan, chitosan nanoparticle and chitosan n-benzaldehyde Schiff base of 00mm – 08mm for both fungi: *Aspergillus niger* and *candida albicans* at different concentrations of 25%, 50% and 100% and also a trend of a high broader spectrum activity, higher inhibition and killing rate of the organisms: *Aspergillus niger* and *candida albicans* to be of the order of chitosan nanoparticle n – benzaldehyde Schiff base < Fe(III) chitosan nanoparticle n – benzaldehyde Schiff base, with inhibition zones ranging from 08mm – 12mm for *Aspergillus niger* and 08mm – 16mm for *Candida albicans* at different concentrations of 25%, 50% and 100%. These activities may be attributed to the structural characteristics of Fe(III) Chitosan nanoparticle n – benzaldehyde Schiff base which is the chelation of the metal ion (Fe(III)) unto the condensation of imine group of chitosan – tpp n – benzaldehyde Schiff base, the enhanced result of the nanoparticle is because of its ease in reaching the target sites of the organism, increase in positive charge density, hydrophilicity, better solubility of the materials in aqueous media of the organism, suppression of spore elements and binding to essential nutrients needed for microbial growth and also the enhanced adsorption of polycation onto the negatively charged cell surface of the micro-organisms [22].

Table 3. The antibacterial activity of the materials (mm) against *Bacillus substilis* (Gram + bacteria).

Materials	100%	50%	25%
Chitosan	10	08	00
Chitosan nanoparticle	12	10	00
Chitosan n – benzaldehyde Schiff base	14	10	00
Fe(III) chitosan n – benzaldehyde Schiff base	16	12	00
Chitosan nanoparticle n – benzaldehyde Schiff base	16	14	00
Fe(III) chitosan nanoparticle n – benzaldehydeSchiff base	18	16	10

Table 4. The antibacterial activity of the materials (mm) against *Bacillus cereus* (Gram + bacteria).

Materials	100%	50%	25%
Chitosan	14	10	08
Chitosan nanoparticle	16	12	10
Chitosan n – benzaldehyde Schiff base	22	20	18
Fe(III) chitosan n – benzaldehyde Schiff base	24	22	10
Chitosan nanoparticle n – benzaldehyde Schiff base	24	22	20
Fe(III) chitosan nanoparticle n – benzaldehyde Schiff base	26	24	20

Table 5. The antibacterial activity of the materials (mm) against *Staphylococcus aureus* (Gram + bacteria).

Materials	100%	50%	25%
Chitosan	16	00	00
Chitosan nanoparticle	16	14	00
Chitosan n – benzaldehyde Schiff base	18	16	14
Fe(III) chitosan n – benzaldehyde Schiff base	20	18	16
Chitosan nanoparticle n – benzaldehyde Schiff base	20	18	14
Fe(III) chitosan nanoparticle n – benzaldehyde Schiff base	24	20	18

Preprints (www.preprints.org) | NOT PEER-REVIEWED | Posted: 17 July 2023 doi:10.20944/preprints202307.1085.v1

Table 6. The antibacterial activity of the materials (mm) against *Samolena* (Gram - bacteria).

Materials	100%	50%	25%
Chitosan	00	00	00
Chitosan nanoparticle	00	00	00
Chitosan n – benzaldehyde Schiff base	00	00	00
Fe(III) chitosan n – benzaldehyde Schiff base	16	12	10
Chitosan nanoparticle n – benzaldehydeSchiff base	16	12	10
Fe(III) chitosan nanoparticle n – benzaldehyde Schiff base	18	14	12

Table 7. The antibacterial activity of thematerials (mm) against *Pseudomonas aeruginosa* (Gram - bacteria).

Materials	100%	50%	25%
Chitosan	14	12	10
Chitosan nanoparticle	16	14	12
Chitosan n – benzaldehyde Schiff base	08	00	00
Fe (III) chitosan n – benzaldehyde Schiff base	10	00	00
Chitosan nanoparticle n – benzaldehyde Schiff base	10	08	00
Fe (III) chitosan nanoparticle n – benzaldehydeSchiff base	12	10	00

Table 8. The antifungal activity of thematerials (mm) against *Asperigillusniger.*

Materials	100%	50%	25%
Chitosan	08	00	00
Chitosan nanoparticle	10	00	00
Chitosan n – benzaldehyde Schiff base	08	08	00
Fe(III) chitosan n – benzaldehyde Schiff base	10	08	00
Chitosan nanoparticle n – benzaldehyde Schiff base	10	08	08
Fe(III) chitosan nanoparticle n – benzaldehyde Schiff base	12	10	08

Table 9. The antifungal activity of thematerials (mm) against *Candida albicans.*

Materials	100%	50%	25%
Chitosan	00	00	00
Chitosan nanoparticle	00	00	00
Chitosan n – benzaldehyde Schiff base	08	00	00
Fe(III) chitosan n – benzaldehyde Schiff base	10	08	00
Chitosan nanoparticle n – benzaldehyde Schiff base	14	12	00
Fe(III) chitosan nanoparticle n – benzaldehyde Schiff base	16	14	08

3.10. Total evaluation of the antimicrobial activities of the produced materials against the various bacteria and fungi:

Results from Tables 5–11, shows that the tested materials exhibited excellent antimicrobial activities against all selected strains and also the materials activities were dependent on the following factors: 1) The structural properties and functional groups of all the materials $–NH_2$, OH, P=O, P-O, C=N and Fe^{3+}, Particle size, Type of organism and Concentration of the inoculates.

Table 10. The antibacterial activity of different standard drugs inhibition zone (mm) against some bacteria.

Bacteria	Standard Drugs Inhibition Zone (mm)							
	CIP	RL	MEM	CN	VA	AMC	CAZ	E
Bacillus subtilis (+)	26	10	12	16	00	00	00	00
Bacillus cereus (+)	28	00	24	00	00	00	14	00

Preprints (www.preprints.org) | NOT PEER-REVIEWED | Posted: 17 July 2023 doi:10.20944/preprints202307.1085.v1

Samolena(-)	28	12	34	00	08	22	08	12
Pseudomonas (-)	36	20	30	24	00	00	28	00
Staphylococcus aureus (+)	24	-	24	24	18	14	10	24

Key: Meropenem (MEM), Gentamicin (CN), Vancomycin (VA), Amoxicillin/ Clavulanic Acid (AMC), Ciprofloxacin (CIP), Sulfamethoxazole/ Trimethoprim (RL), Ceftazidime (CAZ), Erythromycin (E).

Table 11. The antifungal activity of Fluconazole (F) inhibition zone (mm) against *Candida albicans and Aspergillus niger* fungi.

Fungi	Fluconazole Inhibition Zone (mm)
Candida albicans	24
Aspergillus niger	18

3.11. Comparison of the antimicrobial activities of the Gram-positive bacteria against Gram negative bacteria:

It was observed from Tables 3–7 that the materials were more active against the Gram-positive bacteria than the Gram-negative bacteria. The inhibition zone of 18 mm for *Bacillus subtilis* (+), 26 mm for *Bacillus cereus* (+), 24 mm for *Staphylococcus aureus* (+), 18 mm for *Samolena* (-) and 12 mm for *Pseudomonas aeruginosa* (-). This may be attributed to the bacterial cell wall difference. The cell wall of Gram-positive bacteria is fully composed of peptide polyglycogen. The peptidoglycan layer is composed of networks with plenty of pores, which allows foreign molecules to enter into the cell without difficulty and also allow more rapid absorption of ions into the cell. The cell wall of Gram-negative bacteria is made up of bilayer composed cell wall, of a thin membrane of peptide polyglycogen and an outer membrane constituted of lipopolysaccharide, lipoprotein and phospholipids. Due to the bilayer cell membrane of Gram – negative bacteria the outer membrane is a potential barrier against foreign molecules from penetrating the cell wall [9].

3.12. Comparison of the antimicrobial activities of the nanoparticle materials against microparticle materials:

The antimicrobial activities of the nanoparticle materials and microparticle materials were compared in all the Tables 5–11. Obviously, the antimicrobial activities of the nanoparticle materials have better activity than the microparticle materials. This is because nanoparticles have small quantum size effect, large surface area to volume ratio, enhanced solubility, increased rates of dissolution of molecules into microbial cell and also it has the ability to target specific sites of the microbial cells easily than microparticles.

3.13. Comparison of the antimicrobial activities of the synthesized materials against standard drugs:

3.13.1. The experimental results of antimicrobial activity of all the standard drugs using the inhibition zone method:

The antimicrobial activities of Meropenem (MEM), Gentamicin (CN), Vancomycin (VA), Amoxicillin/ Clavulanic Acid (AMC), Ciprofloxacin (CIP), Sulfamethoxazole/ Trimethoprim (RL), Ceftazidime (CAZ), Erythromycin (E) on three Gram positive bacteria: *Bacillus Subtilis*, *Bacillus cereus* and *Staphylococcus aureus*, two Gram-negative bacteria: *Samolena* and *Pseudomonas aeruginosa* and Fluconazole (F) on two fungi: *Candida albicans* and *Aspergillus niger* as shown in plate 3.11, each spot on the plate represents each standard drugs. In a typical experiment, the inhibition zone results were recorded after 24 hours of incubation at 37^0C for bacteria and 3 days of incubation at 37^0C for fungi. The obtained experimental data are clearly shown in Tables 10–11.

From the results above, the antimicrobial activities of the synthesised materials were high for bacteria: *Bacillussubtilis, Bacillus cereus, Staphylococcus aureus, Samolena,Pseudomonas aeruginosa* when compared with the standard drugs: Vancomycin (VA), Amoxicillin/ Clavulanic Acid (AMC), Sulfamethoxazole/ Trimethoprim (RL), Ceftazidime (CAZ), Erythromycin (E). This may be due to each functional group, chemical bond ($–NH_2$, OH, P=O, P-O, C=N and Fe^{3+}) and particle size especially in the nanorange because nanoparticle have small quantum size effect, large surface area

to volume ratio, enhanced solubility, increased rates of dissolution of molecules into microbial cell and also the ability to target specific sites of the microbial cells.

However, it was observed that the materials have similar activities with the following standard drugs: Gentamicin (CN), Ciprofloxacin (CIP), Meropenem (MEM).This may be due to the similarity in functional group and chemical bond present in the materials and the standard drugs- $-NH_2$, OH and C=N. All the antimicrobial activities of the synthesised materials to the fungi: *Candida albicans* and *Aspergillusniger*were less than the standard drug Fluconazole (F) for fungi. This may be due to the functional group and chemical bond (N – N) present in the standard drug. It is known that drugs that contain nitrogen are effective antifungal agents (Kinga et al. 2013; Wikipedia). All results have shown that chitosan, chitosan nanoparticle, chitosan Schiff base, chitosan nanoparticle Schiff base, Fe(III) chitosan Schiff base and Fe(III) chitosan nanoparticle Schiff base are good antimicrobial agents.

5. Conclusion

Chitosan, chitosan nanoparticle, chitosan n – benzaldehyde Schiff base, chitosan nanoparticle n-benzaldehyde Schiff base, Fe(III) chitosan n-benzaldehyde Schiff base and Fe(III) chitosan nanoparticle n-benzaldehyde Schiff base have been synthesized through the reaction of Chitosan with Tpp, Benzaldehyde and Fe^{3+} and characterized by conventional methods: degree of deacetylation, FTIR, SEM and XRD. FTIR results showed a clear variation in the materials produced by indicating the presence of NH_2, OH, P=O, P-O, imine groups and co-ordination reaction in the n-benzaldehyde Schiff base skeleton. The XRD patterns confirmed the change in crystallinity of chitosan derivatives and the SEM images showed increased porosity, particle size/shape of the chitosan derivatives in comparison with chitosan. This was mainly attributed to the formation of chitosan nanoparticle, n-benzaldehyde Schiff base and Fe^{3+} complex with varying electrostatic interaction, hydrogen bond interaction and covalent bonds. The synthesized materials which were screened for their antimicrobial activities against three gram-positive bacteria: *Bacillus subtilis, Bacillus cereus* and *Staphylococcus aureus*, two gram-negative bacteria: *Samolena* and *Pseudomonas aeruginosa* and two fungi: *Candida albicans* and *Aspergillus niger*, were compared against standard drugs: meropenem (MEM), gentamicin (CN), vancomycin (VA), amoxicillin/ clavulanic acid (AMC), ciprofloxacin (CIP), sulfamethoxazole/ trimethoprim (RL), ceftazidime (CAZ), erythromycin (E) for bacteria and fluconazole (F) for fungal. The synthesized materials showed an appreciable high level of antimicrobial activities. The antimicrobial activities of the synthesized materials were dependent on the following factors: The structural functional group properties of all the materials $-NH_2$, OH, P=O, P-O, C=N and Fe^{3+}, particle size, type of organism and concentration of the materials. All results showed that chitosan, chitosan nanoparticle, chitosan n-benzaldehyde Schiff base, chitosan nanoparticle n-benzaldehyde Schiff base, Fe(III) chitosan n – benzaldehyde Schiff base and Fe(III) chitosan nanoparticle n – benzaldehyde Schiff base are good antimicrobial agents.

Compliance with ethical standards:

Acknowledgments: The authors gratefully acknowledge University of Benin, Department of Chemistry and Physics for the support of this project and Delta State University, Abraka

Disclosure of conflict of interest: We declare that we have no conflict of interest.

References

1. Ifeanyi E,Otuokere JC, Anyanwu and Igwe KK (2020). Ni(II) Complex of a Novel Schiff Base Derived from Benzaldehyde and Sulphathiazole: Synthesis, Characterization and Antibacterial Studies. Communication in physical sciences. 145 – 155.
2. Ayodele TO. (2023) Ease to Challenges in Achieving Successful Synthesized Schiff base, Chirality, and Application as Antibacterial Agent. *BioMed Research International.* Volume 2023, Article ID 1626488, 1 – 22.
3. Warra AA (2011). Transition metal complexes and their application in drugs and cosmetics: A Review. *Journal of Chemical and Pharmaceutical Research.* 3(4): 951 – 958.

4. Hernandez M, Angel M, Michael KK, Timothy S, Keizer BC, Yearwood and Atwood DA (2002). Six – coordinate Aluminium cations: characterization, catalysis and theory. *Journal of the Chem. Soc.*, Dalton Trans 3 (410 – 414).
5. Zhikuan Y, Yuting W and Yurong T (1999). Preparation and Adsorption Properties of Metal Ions of Crosslinked Chitosan Azacrown Ethers. *Journal of Applied Polymer Science*, Vol. 74, 3053 – 3058.
6. Muzzerelli RAA., and Peter MG (1997). Some modified chitosans and their niche applications, Chitin handbook. *European Chitin Society, Italy*: 47 – 52.
7. Wu W, He Q and Jiang C (2008). Magnetic Iron Oxide Nanoparticles: Synthesis and Surface Functionalization Strategies.*Nanoscale Research Letter*, 3 (11), 397 – 415
8. Vita TM, Ika OW, Rizky AS, Dionysius JDHS, Akhmad S (2016). In – situ synthesis and characterization of chitosan – Fe_3O_4 nanoparticles using tripolyphosphate/citrate as cross – linker. *Scientific Study & Research.* 17 (3), pp. 249 – 260
9. Nadia AM, Magdy WS, Ahmed HH, El-ghandour MM, Abel-aziz O and Abdel-gawad F (2013). Preparation, characterization and antimicrobial activity of carboxymethyl Chitosan Schiff base with different benzaldehyde derivatives. *Journal of American Science*.**9**(3): 247 – 264.
10. Sashikala S. and Syed S. S (2014). Synthesis and characterisation of chitosan Schiff base derivatives. *Scholars Research Library*.**6** (2): 90 – 97.
11. Knorr D (1982) Functional properties of chitin and chitosan. *Journal of Food Science*: 47(2): 1365 – 2621.
12. Al- Sughayer MA, Muslim SS and Elsabee MZ. (2009). Extraction and characterization of chitin and chitosan from marine sources in Arabian Gulf. *Carbohydrate Polymer* **77**(1): 410 – 419.
13. Mirzadeh H, Yaghobi N, Amanpour S, Ahmadi H, Mohagheni MA and Hormoni F. (2002) Preparation of Chitosan derived from Shrimp shell, Persian Gulf as blood Hemostasis agent. *Iranian Polymer Journal*.**11** (1):63 – 68.
14. Islam MM, Masun SM, Molla MAI, Rahman MM, Shaikh AA and Roy SK (2011). Preparation of Chitosan from shrimp shell and investigation of its properties. *International Journal of Basic and Applied Sciences*.**11**(10):116 – 130
15. Pradip KD, Joydeep D and Tripathy VS (2004). Chitin and Chitosan: Chemistry, properties and applications. *Journal of Science and Industrial Research*.**63**:20
16. Signini R and Campana Filho SP (1999). On the preparation and characterization of chitosan hydrochloride, *Polymer Bulletin*.**42**: 159 – 166.
17. Rajalakshmi, R., Indira, M., Y., Aruna, U., Vinesha, V., Rupangada, V., Krishna M and S.B. (2014). Chitosan Nanoparticles – An emerging trend in nanotechnology. *International Journal of Drug Delivery*; **6**: 204 – 229
18. Morteza HK, Mohammad K, Mobina K and Sahar K (2011). Reinforcement of Chitosan nanoparticles obtained by an Ionic Cross-linking process.*Iranian Polymer Journal*. **20** (5):455-456.
19. Jiao TF, Juan Z, Jingxin Z, Lihua G,YuanyuanX and Xuhui L (2011). Synthesis and Characterization of Chitosan-based Schiff Base Compounds with Aromatic Substituent Groups.*Iranian Polymer Journal*. **20**(2): 123-136.
20. MohyEldin M, Hashem AI, Omer AM and Tamer MT (2015). Preparation, Characterisation and antimicrobial evaluation of novel cinnamyl chitosan Schiff base. *International Journal of Advanced Research*. **3**: 741-755.
21. Semahat K, Zehra OE, Jiri BMS and Nuriye K (2013). A Novel Chitosan Nanoparticle-Schiff Base Modified Carbon Paste Electrode as a Sensor for the Determination of Pb(II) in Waste Water.*Int. J. Electrochem. Sci.* **8**: 2164 – 2181.
22. Xiaohui W, Yumin D, Lihong F, Hui L and Ying H (2005). Chitosan- metal complex as antimicrobial agent: Synthesis, Characterization and Structure–activity study. *Polymer Bulletin*. **55**: 105-113.
23. Alvarenga ES. (2011). Characterization and properties of chitosan in Elnashar PM (ed). *Biotechnology of Biopolymers*.90-109
24. Tran DL, Vu Dinh H, Le Ngoc, Lien, Nguyen NT and Pham GD (2004). Synthesis and Chacterisation of Chitosan nanoparticles Used as Drug Carrier.1-6. https.//Www. Research Gate. Net.
25. Sashikala S and Syed SS (2015). Synthesis, Characterization and Antimicrobial activity of chitosan 4-chlorobenzaldehye Schiff base. *Research Journal of Chemical Sciences*.**5**(9): 27-33.
26. Antony R, TheodoreD, Karuppasamy K, Saravanan K and Thanikaikarasan S. (2012). Structural, Surface, Thermal and Catalytic Properties of Chitosan Supported Cu(II) mixed ligand Complex materials. *Journal of Surface Engineered Materials and advanced technology.* Vol 2(4) 284-291
27. Xia W, Lui P, Zhang J and Chen J (2011). Biological activities of chitosan and chitooligosaccharides. *Food Hydrocolloids*.**25**: 170-179.
28. Enaroseha O. E. Omamoke and E. G. Akpojotor (2013). Superconductivity Driven by Magnetic Instability in CeCu2Si2. Advances in Physics Theories and Application, Vol.18, 54 – 60.
29. Enaroseha O. E. Omamoke, Obed Oyibo, and N. Okpara. (2021). Analysis of Ground State Properties of Interacting Electrons in the Anderson Model. The Journal of Applied Sciences Research, 8(1), 15 – 27.

30. Enaroseha O. E. Omamoke, Obed Oyibo, Damaris Osiga – Aibangbee and Eno Odia (2021). Magnetic Phase Diagram in the Periodic Anderson Model (PAM): An Exact Diagonalization Approach. International Research Journal of Pure and Applied Physics, Vol. 8(1): 14 – 21
31. Enaroseha O. E. Omamoke and N. N. Omehe (2020). Heat Transfer in Circular Tubes with Supercritical Fluid Using the STAR CCM + CFD Code, African Journal of Research in Physical Science 10, 24 – 31.
32. Enaroseha O. E Omamoke, Priscilla O. Osuhor, Obed Oyibo And Ernest O. Ojegu (2021). Theoretical Study of Phonon Spectra in Aluminium (Al) and Copper (Cu): Application of Density Functional Theory and Inter– Atomic Force Constant. Solid State Technology Volume: 64 (2), 1984 - 1999.
33. Enaroseha O. E Omamoke, Obed Oyibo, Priscilla O. Osuhor, Ovie Oghenerhoro (2021). Lattice Dynamics in Some FCC Metals: Application of Phonon Dispersions in Nickel (Ni) and Platinium (Pt). Solid State Technology Volume: 64 (2), 4640 - 4655Omehe N. N. and
34. Enaroseha O. E Omamoke (2019). Ab Initio Investigation of AgGa2 and AgGaSe2. International Journal of Engineering Applied Sciences and Technology, 4 (5), 354 – 360
35. Enaroseha O. Omamoke, O Oyibo, D Osiga–Aibangbee, EM Odia (2021) Magnetic Phase Transition in the Periodic Anderson Model (PAM): An Exact – Diagonalization Approach. International Research Journalof Pure and Applied Physics 8 (1), 14 - 21